Citation for published version:
Kim, Y, Li, S, Phuntsho, S, Xie, M, Shon, HK & Ghaffour, N 2019, 'Understanding the organic micropollutants transport mechanisms in the fertilizer-drawn forward osmosis process', *Journal of Environmental Management*, vol. 248, 109240. https://doi.org/10.1016/j.jenvman.2019.07.011

DOI:
10.1016/j.jenvman.2019.07.011

Publication date:
2019

Document Version
Peer reviewed version

Link to publication

Publisher Rights
CC BY-NC-ND

University of Bath

Alternative formats
If you require this document in an alternative format, please contact:
openaccess@bath.ac.uk

General rights
Copyright and moral rights for the publications made accessible in the public portal are retained by the authors and/or other copyright owners and it is a condition of accessing publications that users recognise and abide by the legal requirements associated with these rights.

Take down policy
If you believe that this document breaches copyright please contact us providing details, and we will remove access to the work immediately and investigate your claim.

Download date: 16. Mar. 2025

Understanding the organic micropollutants transport mechanisms in the fertilizer-drawn forward osmosis process

Youngjin Kim [a], Sheng Li [a,b], Sherub Phuntsho [c], Ming Xie [d], Ho Kyong Shon [c]*, Noreddine Ghaffour [a]*

[a] *King Abdullah University of Science and Technology (KAUST), Water Desalination and Reuse Center (WDRC), Division of Biological & Environmental Science & Engineering (BESE), Thuwal 23955-6900, Saudi Arabia*

[b] *Guangzhou Institute of Advanced Technology, Chinese Academy of Science, Haibin Road #1121, Nansha district, Guangzhou, China*

[c] *Centre for Technology in Water and Wastewater, School of Civil and Environmental Engineering, University of Technology Sydney (UTS), Post Box 129, Broadway, NSW 2007, Australia*

[d] *Department of Chemical Engineering, University of Bath, Claverton Down, Bath BA2 7AY, UK*

[*] *Co-corresponding authors: Ho Kyong Shon, Tel.: +61-2-9514-2629; E-mail: Hokyong.Shon-1@uts.edu.au, Noreddine Ghaffour. Tel. +966-128082180, E-mail: noreddine.ghaffour@kaust.edu.sa*

Graphical abstract

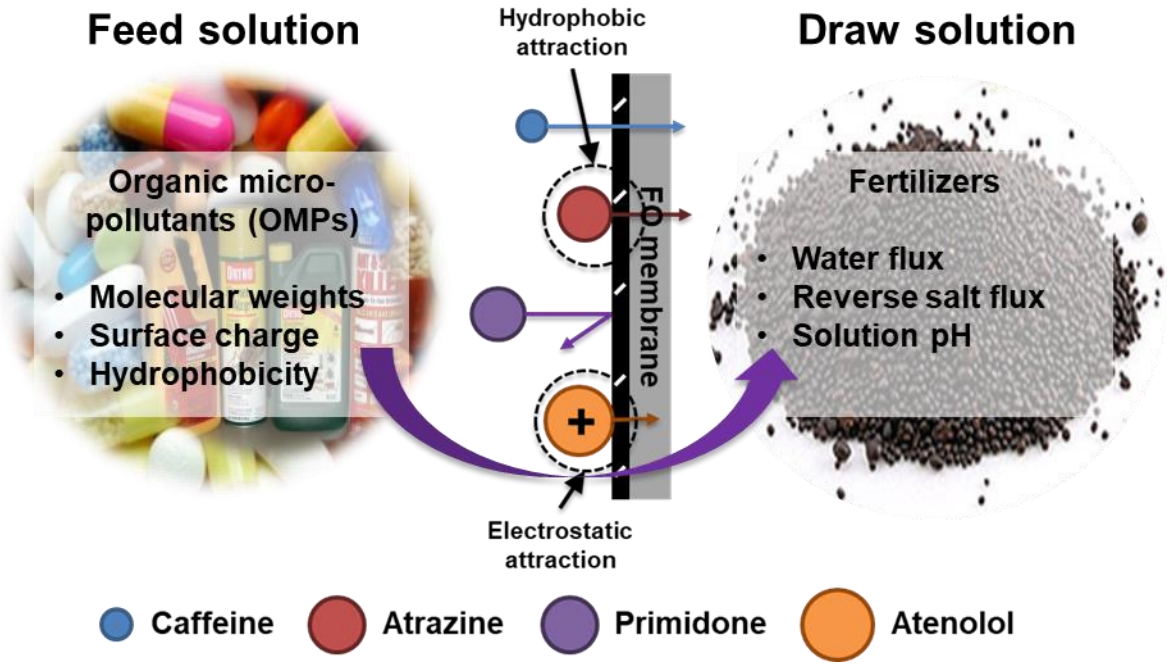

Highlights

- Performance of FDFO was significantly affected by the property of fertilizer DS.

- OMPs transport was governed by physicochemical property at low water flux and RSF.
- DAP reduced OMPs flux due to enhanced steric hindrance by increased FS pH and RSF.
- Transport of OMPs having high molecular weight was readily hampered by high RSF.
- The pore hindrance model could be helpful in understanding OMPs transport in FDFO.

Abstract

We systematically investigated the transport mechanisms of organic micropollutants (OMPs) in a fertilizer-drawn forward osmosis (FDFO) membrane process. Four representative OMPs, i.e., atenolol, atrazine, primidone, and caffeine, were chosen for their different molecular weights and structural characteristics. All the FDFO experiments were conducted with the membrane active layer on the feed solution (FS) side using three different fertilizer draw solutions (DS): potassium chloride (KCl), monoammonium phosphate (MAP), and diammonium phosphate (DAP) due to their different properties (i.e., osmotic pressure, diffusivity, viscosity and solution pH). Using KCl as the DS resulted in both the highest water flux and the highest reverse solute flux (RSF), while MAP and DAP resulted in similar water fluxes with varying RSF. The pH of the FS increased with DAP as the DS due to the reverse diffusion of NH_4^+ ions from the DS toward the FS, while for MAP and DAP DS, the pH of the FS was not impacted. The OMPs transport behavior (OMPs flux) was evaluated and compared with a simulated OMPs flux obtained via the pore-hindrance transport model to identify the effects of the OMPs structural properties. When MAP was used as DS, the OMPs flux was dominantly influenced by the physicochemical properties (i.e., hydrophobicity and surface charge). Those OMPs with positive charge and more hydrophobic, exhibited higher forward OMP fluxes. With DAP as the DS, the more hydrated FO membrane (caused by increased pH) as well as the enhanced RSF hindered OMPs transport through the FO membrane. With KCl as DS, the structural properties of the OMPs were dominant factors in the OMPs flux, however the higher RSF of the KCl draw solute may likely hamper the OMPs transport through the membrane especially those with higher MW (e.g., atenolol). The pore-hindrance model can be instrumental in understanding the effects of the hydrodynamic properties and the surface properties on the OMPs transport behaviors.

Keywords: FDFO; Organic micropollutants; Fertilizer properties; OMPs properties; Pore-hindrance model.

1. Introduction

Organic micropollutants (OMPs), such as pharmaceutical and personal care products, pesticides, herbicides, household chemicals, have become a growing risk to public health and the environment in the past decades (Arslan et al., 2017; Snyder et al., 2003; Tang et al., 2013). Despite the significant possible impact of OMPs, no legal discharge limits have been set by most countries. Only a few countries monitor and manage OMPs discharge through a watch list (Barbosa et al., 2016). While wastewater reuse can sustain freshwater resources and provide necessary nutrients for plants (Jeong et al., 2016), the presence of OMPs in raw sewage (Escher et al., 2014) directly influences and reduces its reuse, particularly in the agricultural sector. A more efficient process for the removal of OMPs from wastewater could facilitate the reuse and discharge of wastewater.

The OMPs removal efficiencies of conventional biological wastewater treatment technologies, such as the activated sludge process, are reported to range from 0% to 90% depending on OMPs properties, sludge properties, and operating conditions (Grandclément et al., 2017). Such variation limits the consistent and safe reuse of wastewater (Bernhard et al., 2006; Carballa et al., 2004; Clara et al., 2005; Grandclément et al., 2017; Pérez et al., 2005). To enhance the efficiency of biological treatments, a membrane bioreactor (MBR), which combined a bioreactor with microfiltration (MF) or ultrafiltration (UF), was proposed (Krzeminski et al., 2017). This MBR advertised a small environmental footprint, high effluent quality, and complete rejection of suspended solids, and could be effective in the treatment of OMPs that were not readily removed by the activated sludge treatment process (Bernhard et al., 2006; Clara et al., 2005; Hai et al., 2011). However, this MBR technology did not meet the permissible limits, e.g., 1 μg L^{-1} for irrigation reuse ((NSW), 2004), for adequate water-reuse quality.

Wastewater reclamation and reuse is considered more cost-effective and environmentally friendly than seawater desalination for solving water-scarcity issues because it has low energy requirements and additional water does not need to be transferred to inland regions (Shannon et al., 2008). Advanced membrane processes, such as nanofiltration (NF) or reverse osmosis (RO), have been widely employed in wastewater reuse to improve the efficiency of OMPs removal, since

even very low concentrations of many OMPs may have a harmful impact on the environment (Fujioka et al., 2015; Radjenović et al., 2008; Snyder et al., 2003). Ionic or charged OMPs are rejected more easily by RO membranes with a negative surface charge, while hydrophobic nonionic OMPs are rejected at decreasing rates with operation (Xu et al., 2005). Also, the rejection of negatively charged OMPs was observed to be higher than that of positively charged OMPs, despite similar molecular weights (Fujioka et al., 2015). While both the NF and RO membranes achieved high rejections of OMPs, they also failed to retain some OMPs, implying that the reuse of wastewater treated with these membranes may pose a risk (Radjenović et al., 2008). Furthermore, pressure-driven membrane-based desalting processes have many disadvantages, e.g., high energy demands and severe membrane fouling caused by high hydraulic pressure (Chong et al., 2015; Ghaffour et al., 2013; Xie et al., 2015).

To overcome these problems, forward osmosis (FO) was recently presented as a potential alternative to the conventional, pressure-driven membrane processes used for desalination (Lee et al., 2010). FO uses a high concentration gradient as its driving force, which not only generates a high water flux, but also reversely diffuses the draw solutes towards the feed solution (FS). As the reverse solute flux (RSF) moves in the opposite direction of the OMPs solute flux, it hinders the OMPs flux. Thus, the FO process was reported to have a higher OMPs removal efficiency than the RO process (Kim et al., 2012; Xie et al., 2012a).

Operational conditions (i.e., water flux, solution pH, membrane orientation, and working temperature) also significantly affect OMPs rejections (Jamil et al., 2016; Jin et al., 2012; Xie et al., 2013). The OMPs removal of the FO process was much less efficient when the active layer of the membrane was facing the draw solution (DS), i.e., AL-DS, than when the active layer was oriented towards the feed solution (FS), i.e., AL-FS (Jin et al., 2012; Xie et al., 2012b). In the AL-FS orientation, an internal concentration polarization (ICP) occurred, which not only increased the OMPs concentration inside the membrane support layer, but also severely restricted the backward diffusion (mass transfer) of the OMPs into the bulk FS. Thus, the OMPs flux was enhanced and the efficiency of its removal was reduced (Alturki et al., 2013; Jin et al., 2012). At high FS temperatures, the OMPs rejection decreased due to the enhanced OMPs diffusivity; the opposite effect was observed at high DS temperatures. The OMPs rejection increased at high DS temperatures because the enhanced water flux had a diluting effect and the slightly elevated reverse

solute flux had a hindrance effect (Xie et al., 2013). The solution pH also significantly influenced the ionic OMPs rejection (Xie et al., 2012b). The thin-film composite (TFC) FO membrane based on polyamide (PA) was reported to have a much better OMPs rejection due to pore hydration than FO membranes based on cellulose triacetate (CTA), even though TFC membranes have larger pore sizes (Xie et al., 2014b). Membrane fouling also significantly influenced OMPs rejection, and a previous study observed that the initial FO water flux played a key role in both membrane fouling and OMPs rejection (Jin et al., 2012; Xie et al., 2014a). Interfacial interactions between foulants and membrane are decisive forces to membrane fouling (Qu et al., 2018; Teng et al., 2019), potentially affecting OMPs rejection. The surface characteristics of the fouling layer in a fouled FO membrane could also influence OMPs rejection (Valladares Linares et al., 2011). The characteristics of the fouling/cake layer may be an important factor affecting OMPs rejection due to their different resistance depending on their composition (Teng et al., 2018; Zhang et al., 2018). However, since the FO process simply converts a concentrated DS into a diluted DS, additional desalting processes are needed to produce pure water while the diluted DS is reconcentrated and regenerated for a sustainable operation (Chekli et al., 2016).

The fertilizer-drawn forward osmosis (FDFO) process has received significant attention because a diluted fertilizer DS can be directly applied in irrigation with no need for DS separation (Kim et al., 2018; Kim et al., 2017d). FDFO was employed in irrigation reuse by integrating it with an anaerobic MBR (AnMBR) (Kim et al., 2016), and was successful in concentrating municipal wastewater (Chekli et al., 2017b). However, one of the major concerns with FDFO is the high reverse diffusion of inorganic fertilizers towards the bioreactor, as it negatively impacts the anaerobic microorganisms, reducing biogas production (Kim et al., 2017a; Li et al., 2017b). Also, biofouling on the osmotic membrane surface is considerably influenced by the properties of the fertilizers used as the DS (Li et al., 2017a). Despite these drawbacks, FDFO was found to be feasible for wastewater treatment, and it has exhibited high OMPs removal during the treatment of AnMBR effluent (Kim et al., 2017c). When commercial hydroponic fertilizer solutions were evaluated for use as the DS, the fertilizer solution diluted by a pilot-scale FDFO system was found to be appropriate for a hydroponic application (Chekli et al., 2017a). Though many studies have attempted to understand the FDFO process for wastewater treatment, the OMPs transport mechanisms in the FDFO process have not yet been well elucidated.

Therefore, the aim of this study is to investigate the transport mechanisms of the OMPs in the FDFO process. Four different OMPs (atenolol, atrazine, primidone, and caffeine) were used to investigate the effects of molecular weight and physicochemical properties such as hydrophobicity and surface charge. Caffeine and primidone were compared due to their different molecular weights and similar surface physicochemical properties (i.e., neutral surface charges and similar hydrophobicity). Atrazine and primidone were examined since they have different hydrophobicities, but similar molecular weights and neutral surface charges. Finally, atenolol was examined to determine the effect of a positive surface charge on the OMPs transport behaviors. For evaluation, three different fertilizers potassium chloride (KCl), monoammonium phosphate, i.e., $NH_4H_2PO_4$ (MAP), and diammonium phosphate, i.e., $(NH_4)_2HPO_4$ (DAP)) were employed as draw solutes in this study because they have the different properties and performances (i.e., water flux, RSF, and a pH change of the FS) as reported the FDFO process (Kim et al., 2017c). To identify the effect of the physicochemical properties of the OMPs surfaces on their transport, the pore-hindrance transport model, which has been utilized to estimate rejections by size exclusion (Rodgers and Miller, 1993), was employed and compared to the experimental data.

2. Materials and methods

2.1. Representative organic micropollutants (OMPs)

Four different OMPs, i.e., atenolol, atrazine, caffeine, and primidone, were provided by Sigma Aldrich in a powder form. Their key physicochemical characteristics are presented in **Table 1**. The diffusivity of the solute was calculated based on the Wilke and Chang equation, while the Stokes-Einstein equation was used to calculate the Stokes radius (Wilke and Chang, 1955). To prepare a 4 g L^{-1} stock solution, 4 mg OMPs were added to 1 mL methanol; the stock solution was stored until use at about 4 °C.

Table 1: Key physicochemical characteristics of the OMPs used in this study.

	Caffeine	Atrazine	Primidone	Atenolol
Application	Stimulant	Herbicide	Anticonvulsant	Beta-blocker
Formula	$C_8H_{10}N_4O_2$	$C_8H_{14}ClN_5$	$C_{12}H_{14}N_2O_2$	$C_{14}H_{22}N_2O_3$
Molecular weight (g/mol)	194	216	218	266
Charge[a] (at pH 6.5)	Neutral	Neutral	Neutral	Positive

Log D[a, b] (at pH 6.5)	-0.63	2.64	0.83	-2.09
pK_a[a]	0.52	2.27	12.26	9.6
Diffusivity[c] ($\times 10^{-10}$ m^2/s)	6.46	6.10	6.07	5.46
Stokes radius[d] (nm)	0.33	0.35	0.35	0.39

[a] Information about the surface charge, Log D, and pKa was adopted from the ChemSpider website (http://www.chemspider.com).
[b] High Log D values indicate high hydrophobicity.
[c] Diffusivity at 20 °C was calculated based on the Wilke and Chang equation (Wilke and Chang, 1955).
[d] Stokes radius was calculated based on the Stokes-Einstein equation (Wilke and Chang, 1955).

166

167 *2.2. FO membrane and draw solutions (DS)*

168 CTA FO membranes from HTI (Hydration Technology Innovations, USA) were used in the
169 present study. The membrane transport parameters were adopted from our previous study (Kim
170 et al., 2016), and are presented in **Table S1**, Supplementary Data. The average pore radius and
171 structural factors of FO membranes (**Table S2**, Supplementary Data) from another study (Xie et
172 al., 2014b) were employed and utilized to solve the pore-hindrance transport model. The surface
173 characteristics of the FO membrane, such as contact angle, zeta potential, and roughness of the
174 selective layer, are presented in **Table 2**. A Sigma 701 microbalance (KSV Instrument Ltd.,
175 Finland) was used to determine the surface contact angle. The zeta potential of the membrane
176 surface was measured using a streaming current electrokinetic analyzer (SurPass, Anton Paar
177 GmbH, Austria). The roughness of the membrane surface was characterized using atomic force
178 microscopy (AFM) (Dimension Icon, Germany). At least three measurements were taken for
179 each membrane sample and the average value was used.

180

181 **Table 2.** Surface characteristics of an HTI CTA FO membrane. The zeta potential was measured
182 at pH 6.5 with 0.01 M KCl as the background electrolyte solution. The contact angle and the
183 roughness were determined at pH 6.5 and room temperature. (Average ± standard deviation)

	Contact angle	Zeta potential	Roughness
CTA FO membrane	79.5 ± 5.2°	-6.87 ± 2.07 mV	13.33 ± 2.89 nm

184

185 Three reagent-grade fertilizers (KCl, MAP and DAP) were used as received from Sigma
186 Aldrich for the DS. The DS was prepared by dissolving an appropriate amount of fertilizer salt in

deionized (DI) water. The thermodynamic properties of the fertilizer chemicals are presented in **Table S3**, Supplementary Data.

2.3. FDFO experimental studies

For all the experimental studies, a lab-scale FO unit consisting of two variable-speed gear pumps (Cole-Parmer, USA), a standard membrane cell, two flow meters, and a balance was used. The FO membrane cell contained two symmetric flow channels (100 mm length × 20 mm width × 3 mm depth) for the FS and DS, and the FO membrane was installed between these two channels. The FO membrane cell was operated at a crossflow rate of 8.5 cm s^{-1} in the direction of the co-current crossflow. The FO process was operated in batch mode, meaning that both the FS and DS were recirculated back to their respective solution tanks, which were maintained at a constant temperature of 20 ± 1 °C using a temperature control system. The experiments were carried out for a duration of 10 hours, using a fertilizer DS (either 1 M or 2 M) with the AL-FS membrane orientation. The OMPs transport mechanism was investigated by adding 10 µL OMPs stock solution (1g L^{-1} each OMPs) into 1 L FS to achieve a 10 µg L^{-1} concentration of each OMP. The change in the diluted DS volume was recorded by placing the DS tank on a digital weighing scale (Mettler Toledo, USA) connected to a PC for data logging; these data were used to calculate the water flux using **Eq. (1)**,

$$J_w = \frac{\Delta V_{DS}}{A_m t} \ , \quad (1)$$

where J_w refers to the measured water flux (L m^{-2} h^{-1}), ΔV_{DS} is the change in DS volume (L) during operation, A_m refers to the membrane area (m^2), and t refers to the operation time (h). After the experiments, the concentrated FS was sampled and analyzed to obtain RSF using **Eq. (2)**,

$$J_s = \frac{\Delta m_{DS}}{A_m t} \ , \quad (2)$$

where J_s refers to RSF (mol m^{-2} h^{-1}) and Δm_{DS} is the change in the mass of the draw solutes in the FS during operation (mol). The detailed experimental procedures are described in our previous studies (Kim et al., 2017c; Kim et al., 2017d).

2.4. Analytical methods for OMPs

The OMPs concentrations were obtained based on methods used in our earlier study (Kim et al., 2017c). After the experiments, 100 mL samples were collected, to which 10 µL isotopes were

added (Cambridge Isotope Laboratories, Inc., USA). The OMPs were removed from the samples using solid-phase extraction (Dione Autotrace 280 and Oasis cartridges). Then, the evaporation for extrated samples was conducted at temperature of 60 °C for 1 hour and LC/MS grade methaol was added in evaporated samples to make 1 mL samples. Finally, the OMPs concentrations were measured using liquid chromatography (Agilent Technology 1260 Infinity LC unit, USA) and mass spectrometry (AB SCIEX QTRAP 5500 mass spectrometer, Applied Biosystems, USA). The recovery ratio (i.e., the ratio of the peak areas before and after extraction) was considered to evaluate the loss of OMPs during the extraction and evaporation processes and to calculate the final concentration of OMPs by multiplying the measured concentrations by the obtained recovery ratio. Then, the OMPs forward flux (toward DS) was derived based on the mass balance for OMPs species (Kim et al., 2012; Kim et al., 2017c) using **Eq. (3)**,

$$J_{OMPs} = \frac{C_{OMPs}(V_{Di}+J_w A_m t)}{A_m t} = \frac{C_{OMPs} V_{Df}}{A_m t} \quad , \quad (3)$$

where C_{OMPs} refers to the concentration of OMPs in the DS (μg L^{-1}), V_{di} and V_{df} are the initial and final DS volumes (L), respectively, and J_{OMPs} refers to the forward flux of the OMPs from the FS toward the DS (μg m^{-2} h^{-1}).

2.5. Models for OMPs transport behaviors

2.5.1. Pore-hindrance transport model

It can be assumed that the FO membrane consisted of several cylindrical capillary tubes with the same radius, where the spherical solute particles can penetrate through these FO membrane pores (Xie et al., 2014b). The pore-hindrance transport model was originally developed to simulate blood flow through individual capillaries (Bungay and Brenner, 1973), but it has also been utilized to estimate rejections by size exclusion in porous membranes for microfiltration and ultrafiltration (Rodgers and Miller, 1993), and the NF [27], RO [43], and FO processes(Nghiem et al., 2004; Xie et al., 2014b; Yoon and Lueptow, 2005). So, the real OMPs rejection was determined using **Eq. (4)** (Nghiem et al., 2004; Xie et al., 2014b),

$$R_r = 1 - \frac{C_p}{C_m} = 1 - \frac{\varphi K_c}{1-exp\left(-P_e(1-\varphi K_c)\right)} \quad , \quad (4)$$

where R_r refers to the real rejection of the FO membrane, C_p is the permeate OMPs concentration (μg L^{-1}), C_m is the OMPs concentration at the membrane surface (μg L^{-1}), K_c is the hydrodynamic

hindrance coefficient for convection, φ is the distribution coefficient, and P_e is the membrane peclet number. The distribution coefficient (**Eq. (5)**) is related to the ratio of the OMPs radius to the membrane pore radius (**Eq. (6)**):

$$\varphi = (1-\lambda)^2 \text{ , (5)}$$

$$\lambda = \frac{r_s}{r_p} \text{ . (6)}$$

The peclet number is defined as the ratio of the convective transport rate to the diffusive transport rate, and can be obtained from **Eq. (7)**,

$$\mathrm{Pe} = \frac{K_c J_w l}{K_d D \varepsilon} \text{ , (7)}$$

where K_d refers to the hydrodynamic hindrance coefficient for diffusion, D refers to the Stokes-Einstein diffusion coefficient ($m^2\ s^{-1}$), l is the active layer thickness (m), and ε refers to the active layer effective porosity. The hydrodynamic hindrance coefficients for convection and diffusion can be determined via **Eq. (8) and (9)**, respectively, which were proposed by Bungay and Brenner (Bungay and Brenner, 1973):

$$K_c = \frac{(2-\varphi)K_s}{2K_t} \text{ , (8)}$$

$$K_d = \frac{6\pi}{K_t} \text{ . (9)}$$

Diffusion may be more dominant than convection in determining the solute transports when λ is close to 1. Details on the calculations of the hydrodynamic hindrance coefficients can be found elsewhere (Bungay and Brenner, 1973; Nghiem et al., 2004; Wang et al., 2014).

2.5.2. Relationship between real rejection and observed rejection

Since the real rejection is relative to the permeate and the active layer concentrations, as suggested by **Eq. (4)**, the observed rejection ($R_o = 1 - c_p/c_f$) must be calculated to obtain the OMPs forward flux. The observed rejection can be obtained from the relationship between the real rejection and the observed rejection, which is readily derived from concentration polarization in film theory (Nghiem et al., 2004) and given by **Eq. (10)**:

$$\ln\frac{(1-R_r)}{R_r} = \ln\frac{(1-R_o)}{R_o} - \frac{J_w}{k} \text{ , (10)}$$

where R_o refers to the observed rejection of the FO membrane and k refers to the mass transfer coefficient related to the concentration polarization effects near the membrane active layer (m s^{-1}). Details on calculations of mass transfer coefficients are given elsewhere (Kim et al., 2017c).

2.5.3. Simulation of OMPs forward flux

To simulate the OMPs forward flux, the OMPs concentrations in the FS and the permeate should be determined first. The change in the volume and OMPs concentration of the FS is calculated using a mass balance based on **Eq. (11)**:

$$\frac{dC_f(t)}{dt} = -\frac{J_w(t)A_m C_p(t)}{V_f(t)} - \frac{C_f(t)}{V_f(t)}\frac{V_f(t)}{dt} \quad , \quad (11)$$

where $C_f(t)$ refers to the OMPs concentration in the FS (μg L^{-1}), $J_w(t)$ refers to the water flux (L m^{-2} h^{-1}), $C_p(t)$ is the permeate OMPs concentration (μg L^{-1}), and $V_f(t)$ refers to the FS volume (L). The water fluxes were obtained from the experimental data (**Eq. (1)**) and the permeate concentrations were obtained from **Eq. (4)**. All parameters varied with respect to operation time. The OMPs concentration in the DS should also be determined to obtain the average OMPs forward flux. Similarly, the change in the volume and OMPs concentration of the DS is calculated from the mass balance using **Eq. (12)**:

$$\frac{dC_d(t)}{dt} = \frac{J_w(t)A_m C_p(t)}{V_d(t)} - \frac{C_d(t)}{V_d(t)}\frac{V_d(t)}{dt} \quad . \quad (12)$$

Then, average OMPs forward flux can be obtained via

$$J_{s,OMPs}(t) = \frac{C_d(t)V_d(t)}{A_m} , \quad (13)$$

where $C_d(t)$ refers to the concentration of OMPs in the DS (μg L^{-1}), $V_d(t)$ is the DS volume (L), and $J_{s,OMPs}(t)$ refers to the average forward OMPs flux (μg m^{-2} L^{-1}).

3. Results and discussion

3.1. FDFO membrane performance

In the present study, we investigated the effects of employing three different fertilizer chemicals (MAP, DAP, and KCl) as the DS in FDFO on the transport mechanisms of OMPs. Our previous study showed that MAP and DAP have similar water fluxes but different RSF, while KCl has a higher water flux and RSF than either MAP or DAP (Kim et al., 2017c). Here, we first conducted FO experiments with each of these fertilizers as the DS. The results shown in **Fig. 1** confirm that

KCl exhibited the highest water flux, while MAP and DAP showed similar water fluxes regardless of the DS concentration, consistent with other studies (Kim et al., 2017c; Phuntsho et al., 2011). As presented in **Table S3**, DAP had the highest osmotic pressure. Therefore, since water flux is governed by the effective osmotic pressure gradient across the active layer, DAP might be expected to have the highest water flux. However, DAP with the lowest diffusion coefficient is expected to create higher ICP effect likely resulting in lower water flux than KCl. Besides the membrane structural parameter (support layer porosity and tortuosity), the diffusion coefficient of the solutes has a significant influence on the severity of ICP effects (McCutcheon and Elimelech, 2006). On the other hand, MAP had a lower water flux than KCl despite their similar osmotic pressures (i.e., 49.85 atm and 43.3 atm for MAP 1 M and KCl 1 M, respectively). This was due to the high diffusivity and low viscosity of KCl compared to the other fertilizers tested as the DS. It has been shown in the past that high diffusivity and low viscosity of the DS reduce ICP in the support layer, thereby increasing the effective concentration gradient and improving the water flux (Kim et al., 2015).

We also investigated RSF for the three DS, as shown in **Fig. 1**. KCl showed the highest RSF, followed by DAP and MAP, at both 1 M and 2 M DS concentrations. This high RSF of KCl could be due to the low ICP discussed above. In addition, KCl has a lower hydrated diameter than either MAP or DAP, which possibly results in high salt permeability (Achilli et al., 2010). Despite the lower diffusivity of DAP (**Table S3**), DAP showed higher RSF than MAP. We attribute this to DAP containing more ions, and particularly ammonium ions (NH_4^+), than MAP. Therefore, even though DAP had a lower effective concentration gradient, more ions existed on the active layer, which induced the high RSF. Furthermore, due to the reverse diffusion of these ammonium ions, the pH of the FS increased during the FDFO operation, consistent with our previous study (Kim et al., 2017c). RSF for the 2 M concentration was proportionately higher than for the 1 M concentration.

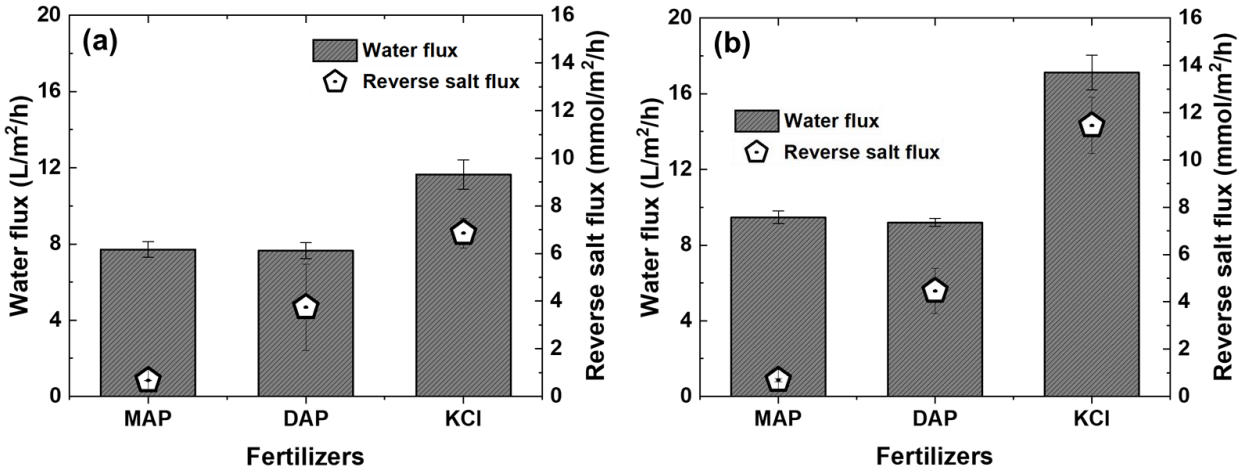

Figure 1. Water flux (columns, left axis) and reverse salt flux (open symbols, right axis) with three fertilizers (MAP, DAP, and KCl) as the DS in FDFO at (a) 1 M DS concentration and (b) 2 M DS concentration.

3.2. OMPs transport behaviors in FDFO

In order to investigate the effects of the physicochemical properties of the OMPs surfaces on their transport behaviors during the FDFO process, we chose to use MAP as the DS. Since MAP had a lower specific RSF (0.1 mmol L^{-1}) compared to the other fertilizers (i.e., 0.3 mmol L^{-1} for DAP and 0.6 mmol L^{-1} for KCl) at 1 M DS concentrations, we expected it to have a smaller impact on the OMPs transport behavior. To evaluate the OMPs transport behaviors, we measured the OMPs forward flux (see **Fig. 2**). Primidone showed the lowest OMPs flux (**Fig. 2a**), followed by caffeine, atenolol, and atrazine. It is well known that OMPs transports in membrane-based processes are dominantly influenced by their molecular weights (Kimura et al., 2004; Kiso et al., 2001; Xie et al., 2014b). However, it was difficult to ascertain a good correlation between the forward OMPs flux and the molecular weight, as shown in **Fig. S1a**. Even though atrazine and atenolol have higher (or similar) molecular weights than caffeine and primidone, the OMPs fluxes of atrazine and atenolol were higher than those of caffeine and primidone. Atrazine in particular exhibited a much higher OMPs flux than primidone despite having a similar molecular weight (i.e., 216 g mol^{-1} and 218 g mol^{-1} for atrazine and primidone, respectively).

When the DS concentration was increased from 1 M to 2 M, as shown in **Fig. 2b**, the OMPs flux slightly decreased (i.e., reduction of 14.2%, 9.2%, and 7.1% for caffeine, atrazine, and primidone, respectively), while the trends among the OMPs did not change significantly. However,

atenolol exhibited a different behavior, as its flux increased by 23.1%, from 18.2 μg m^{-2} h^{-1} to 22.4 μg m^{-2} h^{-1} which is possibly due to its positive charge. When FO process is operated at higher water fluxes using higher DS concentrations, it also proportionately increases the atenolol concentration at the membrane surface due to enhanced ECP effects. This likely enhanced OMP flux of the positively charged atenolol aided by the increased electrostatic attraction with a negatively charged FO membrane surface. Similar to the results at 1 M DS concentration, there was no clear correlation between the molecular weight and the OMPs flux (**Fig. S1b**). These phenomena are likely due to the different physicochemical characteristics (i.e., hydrophobicity and surface charges) of the OMPs.

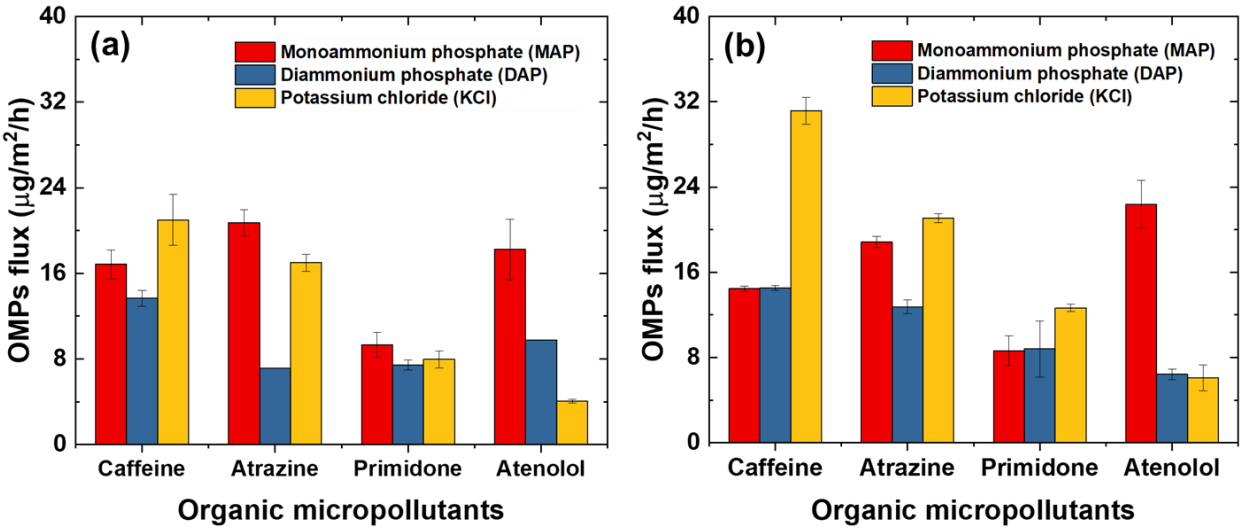

Figure 2. OMPs flux with three fertilizers as the DS (i.e., MAP, DAP, and KCl) during FDFO at (a) 1 M DS concentration and (b) 2 M DS concentration.

To further investigate the effects of the DS properties on the OMPs transport behaviors, we also tested DAP and KCl. As discussed in **Section 3.1**, DAP exhibited a similar water flux but higher RSF than MAP, and KCl showed both a higher water flux and a higher RSF. When using 1 M DAP DS, atrazine exhibited the lowest OMPs flux (**Fig. 2a**) and the highest rejection rate (**Table S4,** Supplementary Data), followed by primidone, atenolol, and caffeine. Compared with 1 M MAP DS, the OMPs fluxes were reduced overall (i.e., reduction ratio: 18.8%, 65.7%, 20.1%, and 46.4% for caffeine, atrazine, primidone, and atenolol, respectively). This might be due to the

combined effects of the enhanced RSF and the increased FS pH on the OMPs transport behaviors, as suggested in **Section 3.1**.

When increasing the DS concentration from 1 M to 2 M, the OMPs fluxes increased by 6.1%, 79.3%, and 18.3% for caffeine, atrazine, and primidone, respectively and while of atenolol, it decreased by 34.3%. This might be due to the enhanced water flux of 9.2 L m^{-2} h^{-1} at 2 M DAP from 7.6 L m^{-2} h^{-1} at 1 M DAP. Increasing the permeation drag force, i.e., water flux, could deteriate the external concentration polarization, thereby increasing the OMPs forward flux. An increase of the atenolol forward flux can be due to slightly higher increase in the feed pH when 2M DAP is used as DS (pH 9.73) compared to 1 M DAP as DS (pH 9.17) due to higher reverse diffusion of NH_4^+ towards the FS at higher DS concentrations. Comparing the DAP DS with the MAP DS, only atrazine and atenolol exhibited noticeable changes in the OMPs forward flux. This result supports the theory that increases in RSF and FS pH have a more significant effect on the transports of hydrophobic and positively charged OMPs.

We conducted FDFO experiments using 1 M KCl as the DS to investigate the effect of RSF on the OMPs transport behaviors. Results show that atenolol exhibited the lowest OMPs flux (4.1 μg^{-1} m^{-2} h^{-1}), followed by primidone, atrazine, and caffeine. The OMPs fluxes of atrazine, primidone, and atenolol were reduced by 18%, 14.4%, and 77.8%, respectively, with 1 M KCl DS compared to 1 M MAP DS, despite the enhanced permeation drag force (50.9%). In contrast, the OMPs flux of caffeine was higher by 24.6% with 1 M KCl DS than with 1 M MAP DS. This may be because the OMPs flux can be dominantly influenced by operational factors, such as water flux, RSF, and physicochemical properties such as molecular size of the OMPs themselves. When the concentration of the KCl DS was increased to 2 M, atenolol had the lowest OMPs flux, followed by primidone, atrazine, and caffeine, similar to the trend seen with 1 M KCl DS (**Fig. 2b**). Therefore, it is interesting to note that the DS with the highest RSF showed a better linear correlation between the OMPs flux and the molecular weight (**Fig. S1**, Supplementary Data).

3.3. Modeling OMPs transports using the pore-hindrance model: Transport mechanisms in FDFO

3.3.1. Effect of OMPs physicochemical properties on OMPs transport behaviors

For a more detailed investigation of the OMPs transport behaviors during the FDFO process, we simulated the OMPs forward fluxes via the pore-hindrance model and the mass balance, and

compared the simulation results with the experimental data. To elucidate the effect of physicochemical properties on the OMPs transports, we modeled the OMPs forward flux with 1 M MAP DS (**Fig. 3a**). Interestingly, the forward fluxes of all the OMPs were increased in the simulations compared to the experiments because the pore-hindrance model considers only the steric hindrance between the OMPs and the FO membrane; their chemical properties were not taken into account. The results presented in the table in **Fig. 3a** show that atrazine and atenolol exhibited more significant differences between their modeled and experimental OMPs fluxes than caffeine and primidone, possibly because of their different physicochemical properties (i.e., hydrophobicity and surface charges) (**Fig. 4a**). The surfaces of caffeine, atrazine, and primidone have similar neutral charges but different hydrophobicities (**Table 1**). Atrazine has a hydrophobic property and this could possibly cause adsorption of atrazine onto the membrane surface, thus, enhancing OMPs transport through the moderately hydrophilic FO membrane (the contact angle of the FO membrane's active layer was 79.5◦ as shown in **Table 2**).To further confirm this hypothesis, we calculated the adsorbed amounts of OMPs based on their mass balance; the results are presented in **Table 3**. Atrazine, which has a neutrally charged surface, exhibited the second highest adsorbed amount (i.e., 2.79 mg m^{-2}, 0.17 mg m^{-2}, 1.27 mg m^{-2}, and 3.31 mg m^{-2} for atrazine, caffeine, primidone, and atenolol, respectively), which resulted in a higher concentration of OMPs in the AL. Therefore, it held true that the hydrophobic interaction could be the dominant mechanism for the transport behavior of atrazine. When the surface hydrophobicity was similar (i.e., caffeine and primidone), caffeine showed a higher OMPs flux than primidone, implying that the molecular weight was the dominant factor determining the forward flux of the OMPs.

Table 3. Adsorbed amounts of OMPs on the membrane surface. Adsorbed amounts of OMPs were estimated via simple mass balance.

	Caffeine	Atrazine	Primidone	Atenolol
Adsorbed amount (mg m^{-2})	0.17	2.79	1.27	3.31

In addition to hydrophobicity, the surface charges of OMPs can seriously influence their transport behavior via electrostatic repulsion or electrostatic attraction with electrically charged membranes (Xie et al., 2012b). **Fig. 2a** shows a higher forward flus for atenolol despite its high

molecular weight and this might be due to the electrostatic attraction caused by the positively charged atenolol OMP and the negatively charged surface of the FO membrane, as shown in **Table 1** and **Table 2**. In **Table 3**, we see that atenolol had the highest amount of OMPs (3.31 mg m^{-2}) adsorbed on the membrane surface. This could have induced a high OMPs concentration gradient across the active layer, thereby enhancing the forward flux of atrazine. When the MAP DS concentration was increased to 2 M from 1 M, the forward flux of atenolol was enhanced, which can be explained due to enhanced ECP when FO is operated at higher water fluxes. This enhanced atenolol concentration at the membrane surface increases its forward flux further aided by the electrostatic attraction between the positively charged atenolol and negatively charged membrane surface. Although the concentrations of the other OMPs also increases at the membrane surface when the FO is operated at higher flux (higher ECP) however, their forward flux decreased which is a rather unexpected behavior since forward solute fluxes are generally a function of its concentration at the membrane surface. Hence, a further studies is required to gain better understanding of why the forward fluxes of other OMPs behave differently when MAP DS is operated at higher concentrations.

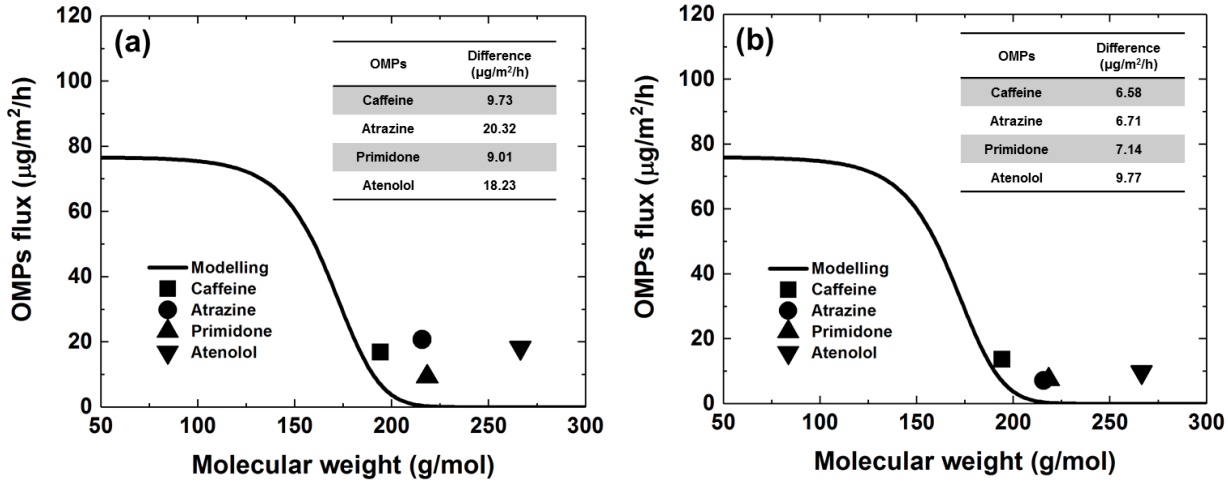

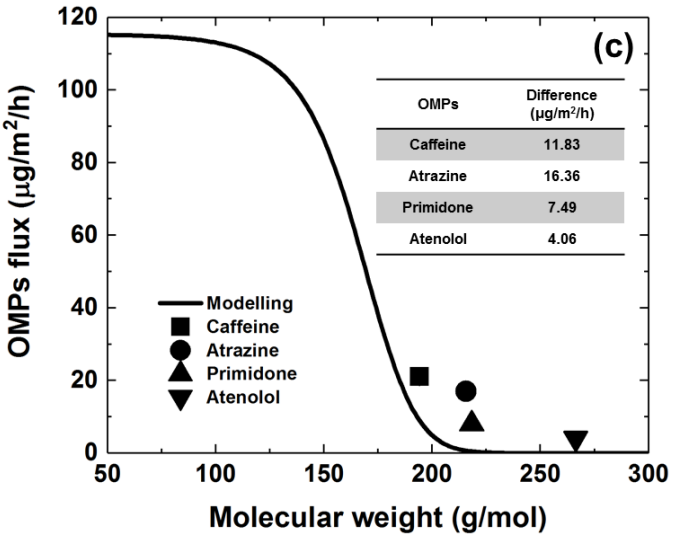

Figure 3. Model predictions (solid line) for OMPs flux with the varying solute molecular weight simulated by the pore-hindrance transport model for (a) MAP DS, (b) DAP DS, and (c) KCl DS at 1 M DS concentration. Also included are the measured solute forward fluxes of the OMPs: caffeine, atrazine, primidone, and atenolol. Tables in each panel indicate the difference between the modeled OMPs flux and the experimental data. The relevant parameters from **Table 1** and **Table S2** were employed for the model calculation; other parameters were adopted from the experimental data presented in **Fig. 1a**.

3.3.2. Effect of alkaline fertilizer (DAP) DS on OMPs transport behaviors

We also investigated the effect of an alkaline fertilizer DS (in this case, we used DAP) on the transport behavior of OMPs during FDFO. An OMPs flux with 1 M DAP DS was simulated using the experimental average water flux, presented in **Fig. 3b**. The differences between the modeled OMPs flux and the experimental data were reduced for all the OMPs, but the forward fluxes of atrazine and atenolol decreased compared to 1 M MAP DS. This could be due to the enhanced RSF combined with a similar water flux (Xie et al., 2012a). The DAP DS had a higher RSF (i.e., 2.5 mmol $m^{-2} h^{-1}$ and 0.7 mmol $m^{-2} h^{-1}$, respectively) than the MAP DS, while the water flux was very similar (i.e., 7.6 L $m^{-2} h^{-1}$ and 7.7 L $m^{-2} h^{-1}$, respectively) as shown in **Fig. 1a**. A high RSF might hinder the transport of feed solutes through the FO membrane, resulting in a lower OMPs forward flux. In addition, the FS pH of the DAP DS increased from 7.05 to 9.17 during 10 h of operation; this could potentially change the membrane surface properties (e.g., by decreasing the

contact angle and slightly increasing the zeta potential) of the FO membrane due to hydrophilic surface functional groups (Xie et al., 2012b) as well as the surface charge of atenolol because of its pKa value of 9.6. Particularly, a reduced contact angle would suggest hydration swelling of the active layer (Ahmad et al., 2008). In this case, atrazine would not reach the FO membrane due to steric hindrance by the water molecules on the membrane surface, making hydrophobic interaction negligible (**Fig. 4b**). As a result, OMPs (i.e., atrazine and primidone) with similar molecular weights but different surface properties exhibited a similar OMPs flux.

For atenolol, we hypothesized that the increase in FS pH from 7.05 to 9.17, resulting in a pKa value of 9.6, changed the surface charge from positive to neutral while other OMPs maintained their surface charge properties. Therefore, atenolol was less adsorbed on the active layer and less likely to be transported into the DS (**Fig. 4b**). To verify this hypothesis, we calculated the adsorbed amounts of atenolol via the mass balance as 3.31 mg m^{-2} and 2.27 mg m^{-2} for MAP 1 M and DAP 1 M, respectively. These amounts were similar to those of another study that found atenolol adsorption (the retardation factor) on a sandy aquifer material was reduced from 23.3 to 15.8 when pH was increased from 4 to 8 (Schaffer et al., 2012).

By simulating the OMPs flux with 2 M DAP DS using the experimental average water flux (**Fig. S2b**), we found that the OMPs transport behavior was dominantly influenced by enhanced steric hindrance. Besides, FS pH became 9.73 higher than that of DAP 1 M DS (pH 9.17), which further reduced the forward flux of atenolol by 34.3%. At higher pH, the atenolol loses its positive charge to become neutral thereby reducing the electrostatic attraction between the atenolol and charged membrane surface and hence lowering its forward flux. This is evident from the consistent trends shown in **Fig. S2b** and **Fig. 3b**, which implicate the increased RSF and a change in the surface properties of both the FO membrane and the OMPs resulting from the increased pH of the FS.

3.3.3. Effect of DS with high RSF (KCl) on OMPs transport behaviors

Lastly, we simulated the OMPs flux with 1 M KCl DS using experimental data and found a high water flux and high RSF. The modeled OMPs flux was noticeably increased with the KCl DS compared to the MAP DS and DAP DS. This was due to the high water flux of the KCl DS compared to the MAP and DAP DS. When comparing the modeled OMPs flux with the

497 experimental OMPs flux, atenolol exhibited the smallest difference, followed by primidone,
498 caffeine, and atrazine (**Fig. 3c**), indicating that the OMPs with high molecular weights were more
499 easily influenced by a high RSF. Therefore, we hypothesized that the forward fluxes of the OMPs
500 were dominantly determined by the interplay among the water flux, RSF, and molecular size of
501 the OMPs. A high water flux causes enhanced external concentration polarization, potentially
502 leading to an increased OMPs flux (Kim et al., 2017b). Hence, caffeine, which has a low molecular
503 weight, may be more easily transferred to the DS than OMPs of higher weight. In addition, the
504 transport of the OMPs was significantly influenced by their molecular weights due to the hindrance
505 effect of a high RSF, as shown in **Fig. 4c**. Consequently, the forward flux of OMPs with high
506 molecular weights became lower in 1 M KCl DS than in 1 M MAP DS. **Fig. S1e** indicates that the
507 forward OMPs flux was a function of molecular weight when using 1 M KCl DS.
508 To validate this hypothesis, we compared the OMPs forward fluxes of 2 M KCl DS (**Fig. S1f**)
509 and 2 M MAP DS (**Fig. S1b**). The results show that the forward fluxes of all the OMPs except
510 atenolol were increased, supporting the hypothesis that the transport of OMPs with a high
511 molecular weight is more affected by RSF than a high water flux. The removal rates of all the
512 OMPs were increased with the KCl DS compared to the MAP DS (**Table S4**). This result agrees
513 well with the results from other studies that a high water flux leads to a decrease in removal rates
514 due to the dilution effect (Lee et al., 2004; Xie et al., 2013). Interestingly, the trends of the three
515 OMPs with neutral surfaces (caffeine, atrazine, and primidone) with the KCl DS were similar to
516 the trends with the MAP DS, but not the DAP DS. The reverse diffusion of the KCl DS did not
517 influence the FS pH and, therefore, the surface chemical properties of the FO membrane were a
518 governing factor in the transport of OMPs with a relatively low molecular weight.
519 The findings from the present study have significant implications for optimizing the FDFO
520 process for treating wastewater that contains OMPs. When using MAP or KCl as the DS, the
521 rejection of the OMPs was governed by the physicochemical properties of their surfaces. However,
522 the DAP DS effectively rejected most of the OMPs due to the increased pH of the FS, which was
523 caused by the backward diffusion of NH_4^+ in the DS. This implies that an alkaline DS is
524 recommended for the effective removal of OMPs from wastewater. We found that the
525 experimental OMPs fluxes were higher than the theoretical OMPs fluxes obtained from the pore-
526 hindrance model. This discrepancy is due to the solution-diffusion model being dominant for non-

porous membranes such as NF, RO, and FO membranes. Nevertheless, because the pore-hindrance model considers only the steric hindrance effect by size exclusion, it still helps us to understand how the surface properties of the OMPs and the FO membrane influenced the OMPs transport behaviors.

4. Conclusion

We systematically investigated the OMPs transport mechanisms in FDFO using four different OMPs with different molecular weights and surface physicochemical characteristics and three different fertilizers as the DS. The transport behaviors of the OMPs were simulated using the pore-hindrance transport model in order to identify the effect of the physicochemical properties of the OMPs surfaces on their transport. The main findings drawn from the present study can be summarized briefly as follows:

- KCl showed the highest water flux and RSF; MAP and DAP exhibited similar water fluxes but different RSF.
- When using either the MAP or KCl DS (which had a moderate water flux and low RSF), the physicochemical properties (i.e., hydrophobicity and surface charge) of the OMPs determined their transport behavior. However, the remarkably increased RSF caused by using KCl as the DS could hamper the transport of OMPs with high molecular weights.
- With the DAP DS, the FO membrane was more hydrated because of the increased pH. RSF was also enhanced, which may have helped prevent the transport of OMPs through the FO membrane. Thus, rejection of all the tested OMPs was enhanced.
- The pore-hindrance model was instrumental in understanding the effects of the hydrodynamic properties and the physicochemical properties on OMPs transports.

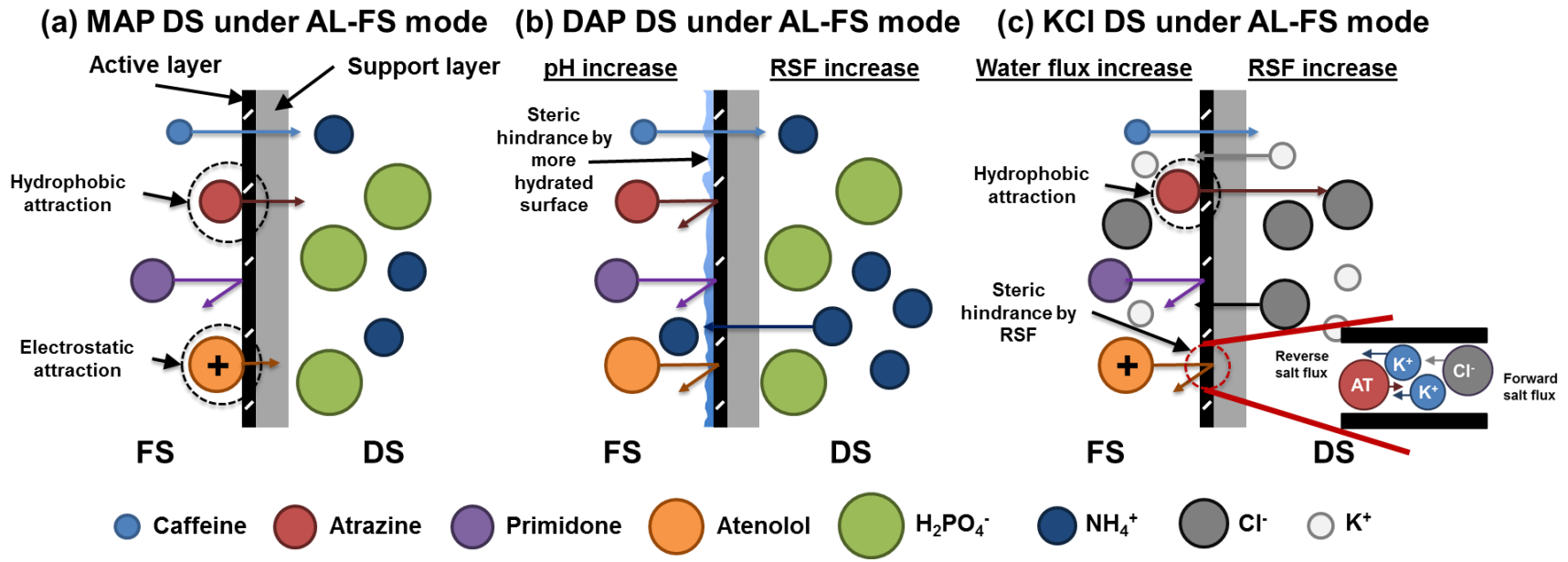

Figure 4. Schematic descriptions of OMPs transport mechanisms in FO. RSF plays an important role in determining the OMPs transports. With MAP DS, which has low RSF, the OMPs transports are dominantly influenced by their properties (i.e., molecular weights, surface charges, and surface hydrophobicity). With DAP DS, which has an intermediate RSF, an increase in FS pH alters the surface physicochemical properties of both the FO membrane and the OMPs; hence, the OMPs transport was significantly influenced. With KCl DS, which has a high RSF, the transport behavior of the OMPs was affected by both the high RSF and the surface properties of OMPs.

Acknowledgements

The research reported in this publication was supported by funding from King Abdullah University of Science and Technology (KAUST). The support of the staff at the KAUST Water Desalination & Reuse Center (WDRC) is also greatly appreciated.

References

(NSW), D.o.E.a.C., 2004. Environmental Guidelines: Use of Effluent by Irrigation. Department of Environment and Conservation (NSW).

Achilli, A., Cath, T.Y., Childress, A.E., 2010. Selection of inorganic-based draw solutions for forward osmosis applications. Journal of Membrane Science 364, 233-241.

Ahmad, A.L., Tan, L.S., Abd. Shukor, S.R., 2008. The role of pH in nanofiltration of atrazine and dimethoate from aqueous solution. Journal of Hazardous Materials 154, 633-638.

Alturki, A.A., McDonald, J.A., Khan, S.J., Price, W.E., Nghiem, L.D., Elimelech, M., 2013. Removal of trace organic contaminants by the forward osmosis process. Separation and Purification Technology 103, 258-266.

Arslan, M., Ullah, I., Müller, J.A., Shahid, N., Afzal, M., 2017. Organic Micropollutants in the Environment: Ecotoxicity Potential and Methods for Remediation, in: Anjum, N.A., Gill, S.S., Tuteja, N. (Eds.), Enhancing Cleanup of Environmental Pollutants: Volume 1: Biological Approaches. Springer International Publishing, Cham, pp. 65-99.

Barbosa, M.O., Moreira, N.F.F., Ribeiro, A.R., Pereira, M.F.R., Silva, A.M.T., 2016. Occurrence and removal of organic micropollutants: An overview of the watch list of EU Decision 2015/495. Water Research 94, 257-279.

Bernhard, M., Müller, J., Knepper, T.P., 2006. Biodegradation of persistent polar pollutants in wastewater: Comparison of an optimised lab-scale membrane bioreactor and activated sludge treatment. Water Research 40, 3419-3428.

Bungay, P.M., Brenner, H., 1973. The motion of a closely-fitting sphere in a fluid-filled tube. International Journal of Multiphase Flow 1, 25-56.

Carballa, M., Omil, F., Lema, J.M., Llompart, M.a., García-Jares, C., Rodríguez, I., Gómez, M., Ternes, T., 2004. Behavior of pharmaceuticals, cosmetics and hormones in a sewage treatment plant. Water Research 38, 2918-2926.

Chekli, L., Kim, J.E., El Saliby, I., Kim, Y., Phuntsho, S., Li, S., Ghaffour, N., Leiknes, T., Kyong Shon, H., 2017a. Fertilizer drawn forward osmosis process for sustainable water reuse to grow hydroponic lettuce using commercial nutrient solution. Separation and Purification Technology 181, 18-28.

Chekli, L., Kim, Y., Phuntsho, S., Li, S., Ghaffour, N., Leiknes, T., Shon, H.K., 2017b. Evaluation of fertilizer-drawn forward osmosis for sustainable agriculture and water reuse in arid regions. Journal of Environmental Management 187, 137-145.

Chekli, L., Phuntsho, S., Kim, J.E., Kim, J., Choi, J.Y., Choi, J.-S., Kim, S., Kim, J.H., Hong, S., Sohn, J., Shon, H.K., 2016. A comprehensive review of hybrid forward osmosis systems: Performance, applications and future prospects. Journal of Membrane Science 497, 430-449.

Chong, T.H., Loo, S.-L., Krantz, W.B., 2015. Energy-efficient reverse osmosis desalination process. Journal of Membrane Science 473, 177-188.

Clara, M., Strenn, B., Gans, O., Martinez, E., Kreuzinger, N., Kroiss, H., 2005. Removal of selected pharmaceuticals, fragrances and endocrine disrupting compounds in a membrane bioreactor and conventional wastewater treatment plants. Water Research 39, 4797-4807.

Escher, B.I., Allinson, M., Altenburger, R., Bain, P.A., Balaguer, P., Busch, W., Crago, J., Denslow, N.D., Dopp, E., Hilscherova, K., Humpage, A.R., Kumar, A., Grimaldi, M., Jayasinghe, B.S., Jarosova, B., Jia, A., Makarov, S., Maruya, K.A., Medvedev, A., Mehinto, A.C., Mendez, J.E., Poulsen, A., Prochazka, E., Richard, J., Schifferli, A., Schlenk, D., Scholz, S., Shiraishi, F., Snyder, S., Su, G., Tang, J.Y.M., Burg, B.v.d., Linden, S.C.v.d., Werner, I., Westerheide, S.D., Wong, C.K.C., Yang, M., Yeung, B.H.Y., Zhang, X., Leusch, F.D.L., 2014. Benchmarking Organic Micropollutants in Wastewater, Recycled Water and Drinking Water with In Vitro Bioassays. Environmental Science & Technology 48, 1940-1956.

Fujioka, T., Khan, S.J., McDonald, J.A., Nghiem, L.D., 2015. Rejection of trace organic chemicals by a nanofiltration membrane: the role of molecular properties and effects of caustic cleaning. Environmental Science: Water Research & Technology 1, 846-854.

Ghaffour, N., Missimer, T.M., Amy, G.L., 2013. Technical review and evaluation of the economics of water desalination: Current and future challenges for better water supply sustainability. Desalination 309, 197-207.

Grandclément, C., Seyssiecq, I., Piram, A., Wong-Wah-Chung, P., Vanot, G., Tiliacos, N., Roche, N., Doumenq, P., 2017. From the conventional biological wastewater treatment to hybrid processes, the evaluation of organic micropollutant removal: A review. Water Research 111, 297-317.

Hai, F.I., Tessmer, K., Nguyen, L.N., Kang, J., Price, W.E., Nghiem, L.D., 2011. Removal of micropollutants by membrane bioreactor under temperature variation. Journal of Membrane Science 383, 144-151.

Jamil, S., Jeong, S., Vigneswaran, S., 2016. Application of pressure assisted forward osmosis for water purification and reuse of reverse osmosis concentrate from a water reclamation plant. Separation and Purification Technology 171, 182-190.

Jeong, H., Seong, C., Jang, T., Park, S., 2016. Classification of Wastewater Reuse for Agriculture: A Case Study in South Korea. Irrigation and Drainage 65, 76-85.

Jin, X., She, Q., Ang, X., Tang, C.Y., 2012. Removal of boron and arsenic by forward osmosis membrane: Influence of membrane orientation and organic fouling. Journal of Membrane Science 389, 182-187.

Kim, C., Lee, S., Shon, H.K., Elimelech, M., Hong, S., 2012. Boron transport in forward osmosis: Measurements, mechanisms, and comparison with reverse osmosis. Journal of Membrane Science 419-420, 42-48.

Kim, J.E., Phuntsho, S., Ali, S.M., Choi, J.Y., Shon, H.K., 2018. Forward osmosis membrane modular configurations for osmotic dilution of seawater by forward osmosis and reverse osmosis hybrid system. Water Research 128, 183-192.

Kim, Y., Chekli, L., Shim, W.-G., Phuntsho, S., Li, S., Ghaffour, N., Leiknes, T., Shon, H.K., 2016. Selection of suitable fertilizer draw solute for a novel fertilizer-drawn forward osmosis–anaerobic membrane bioreactor hybrid system. Bioresource Technology 210, 26-34.

Kim, Y., Lee, S., Shon, H.K., Hong, S., 2015. Organic fouling mechanisms in forward osmosis membrane process under elevated feed and draw solution temperatures. Desalination 355, 169-177.

Kim, Y., Li, S., Chekli, L., Phuntsho, S., Ghaffour, N., Leiknes, T., Shon, H.K., 2017a. Influence of fertilizer draw solution properties on the process performance and microbial community structure in a side-stream anaerobic fertilizer-drawn forward osmosis – ultrafiltration bioreactor. Bioresource Technology 240, 149-156.

Kim, Y., Li, S., Chekli, L., Woo, Y.C., Wei, C.-H., Phuntsho, S., Ghaffour, N., Leiknes, T., Shon, H.K., 2017b. Assessing the removal of organic micro-pollutants from anaerobic membrane bioreactor effluent by fertilizer-drawn forward osmosis. Journal of Membrane Science 533, 84-95.

Kim, Y., Li, S., Chekli, L., Woo, Y.C., Wei, C.-H., Phuntsho, S., Ghaffour, N., Leiknes, T., Shon, H.K., 2017c. Assessing the removal of organic micro-pollutants from anaerobic membrane bioreactor effluent by fertilizer-drawn forward osmosis. Journal of Membrane Science 533, 84-95.

Kim, Y., Woo, Y.C., Phuntsho, S., Nghiem, L.D., Shon, H.K., Hong, S., 2017d. Evaluation of fertilizer-drawn forward osmosis for coal seam gas reverse osmosis brine treatment and sustainable agricultural reuse. Journal of Membrane Science 537, 22-31.

Kimura, K., Toshima, S., Amy, G., Watanabe, Y., 2004. Rejection of neutral endocrine disrupting compounds (EDCs) and pharmaceutical active compounds (PhACs) by RO membranes. Journal of Membrane Science 245, 71-78.

Kiso, Y., Sugiura, Y., Kitao, T., Nishimura, K., 2001. Effects of hydrophobicity and molecular size on rejection of aromatic pesticides with nanofiltration membranes. Journal of Membrane Science 192, 1-10.

Krzeminski, P., Leverette, L., Malamis, S., Katsou, E., 2017. Membrane bioreactors – A review on recent developments in energy reduction, fouling control, novel configurations, LCA and market prospects. Journal of Membrane Science 527, 207-227.

Lee, S., Amy, G., Cho, J., 2004. Applicability of Sherwood correlations for natural organic matter (NOM) transport in nanofiltration (NF) membranes. Journal of Membrane Science 240, 49-65.

Lee, S., Boo, C., Elimelech, M., Hong, S., 2010. Comparison of fouling behavior in forward osmosis (FO) and reverse osmosis (RO). Journal of Membrane Science 365, 34-39.

Li, S., Kim, Y., Chekli, L., Phuntsho, S., Shon, H.K., Leiknes, T., Ghaffour, N., 2017a. Impact of reverse nutrient diffusion on membrane biofouling in fertilizer-drawn forward osmosis. Journal of Membrane Science 539, 108-115.

Li, S., Kim, Y., Phuntsho, S., Chekli, L., Shon, H.K., Leiknes, T., Ghaffour, N., 2017b. Methane production in an anaerobic osmotic membrane bioreactor using forward osmosis: Effect of reverse salt flux. Bioresource Technology 239, 285-293.

McCutcheon, J.R., Elimelech, M., 2006. Influence of concentrative and dilutive internal concentration polarization on flux behavior in forward osmosis. Journal of Membrane Science 284, 237-247.

Nghiem, L.D., Schäfer, A.I., Elimelech, M., 2004. Removal of Natural Hormones by Nanofiltration Membranes: Measurement, Modeling, and Mechanisms. Environmental Science & Technology 38, 1888-1896.

Pérez, S., Eichhorn, P., Aga, D.S., 2005. Evaluating the biodegradability of sulfamethazine, sulfamethoxazole, sulfathiazole, and trimethoprim at different stages of sewage treatment. Environmental Toxicology and Chemistry 24, 1361-1367.

Phuntsho, S., Shon, H.K., Hong, S., Lee, S., Vigneswaran, S., 2011. A novel low energy fertilizer driven forward osmosis desalination for direct fertigation: Evaluating the performance of fertilizer draw solutions. Journal of Membrane Science 375, 172-181.

Qu, X., Cai, X., Zhang, M., Lin, H., Leihong, Z., Liao, B.-Q., 2018. A facile method for simulating randomly rough membrane surface associated with interface behaviors. Applied Surface Science 427, 915-921.

Radjenović, J., Petrović, M., Ventura, F., Barceló, D., 2008. Rejection of pharmaceuticals in nanofiltration and reverse osmosis membrane drinking water treatment. Water Research 42, 3601-3610.

Rodgers, V.G.J., Miller, K.D., 1993. Analysis of steric hindrance reduction in pulsed protein ultrafiltration. Journal of Membrane Science 85, 39-58.

Schaffer, M., Boxberger, N., Börnick, H., Licha, T., Worch, E., 2012. Sorption influenced transport of ionizable pharmaceuticals onto a natural sandy aquifer sediment at different pH. Chemosphere 87, 513-520.

Shannon, M.A., Bohn, P.W., Elimelech, M., Georgiadis, J.G., Mariñas, B.J., Mayes, A.M., 2008. Science and technology for water purification in the coming decades. Nature 452, 301.

Snyder, S.A., Westerhoff, P., Yoon, Y., Sedlak, D.L., 2003. Pharmaceuticals, Personal Care Products, and Endocrine Disruptors in Water: Implications for the Water Industry. Environmental Engineering Science 20, 449-469.

Tang, J.Y.M., McCarty, S., Glenn, E., Neale, P.A., Warne, M.S.J., Escher, B.I., 2013. Mixture effects of organic micropollutants present in water: Towards the development of effect-based water quality trigger values for baseline toxicity. Water Research 47, 3300-3314.

Teng, J., Shen, L., Yu, G., Wang, F., Li, F., Zhou, X., He, Y., Lin, H., 2018. Mechanism analyses of high specific filtration resistance of gel and roles of gel elasticity related with membrane fouling in a membrane bioreactor. Bioresource technology 257, 39-46.

Teng, J., Zhang, M., Leung, K.-T., Chen, J., Hong, H., Lin, H., Liao, B.-Q., 2019. A unified thermodynamic mechanism underlying fouling behaviors of soluble microbial products (SMPs) in a membrane bioreactor. Water Research 149, 477-487.

Valladares Linares, R., Yangali-Quintanilla, V., Li, Z., Amy, G., 2011. Rejection of micropollutants by clean and fouled forward osmosis membrane. Water Research 45, 6737-6744.

Wang, J., Dlamini, D.S., Mishra, A.K., Pendergast, M.T.M., Wong, M.C.Y., Mamba, B.B., Freger, V., Verliefde, A.R.D., Hoek, E.M.V., 2014. A critical review of transport through osmotic membranes. Journal of Membrane Science 454, 516-537.

Wilke, C.R., Chang, P., 1955. Correlation of diffusion coefficients in dilute solutions. AIChE Journal 1, 264-270.

Xie, M., Lee, J., Nghiem, L.D., Elimelech, M., 2015. Role of pressure in organic fouling in forward osmosis and reverse osmosis. Journal of Membrane Science 493, 748-754.

Xie, M., Nghiem, L.D., Price, W.E., Elimelech, M., 2012a. Comparison of the removal of hydrophobic trace organic contaminants by forward osmosis and reverse osmosis. Water Research 46, 2683-2692.

Xie, M., Nghiem, L.D., Price, W.E., Elimelech, M., 2014a. Impact of organic and colloidal fouling on trace organic contaminant rejection by forward osmosis: Role of initial permeate flux. Desalination 336, 146-152.

Xie, M., Nghiem, L.D., Price, W.E., Elimelech, M., 2014b. Relating rejection of trace organic contaminants to membrane properties in forward osmosis: Measurements, modelling and implications. Water Research 49, 265-274.

Xie, M., Price, W.E., Nghiem, L.D., 2012b. Rejection of pharmaceutically active compounds by forward osmosis: Role of solution pH and membrane orientation. Separation and Purification Technology 93, 107-114.

Xie, M., Price, W.E., Nghiem, L.D., Elimelech, M., 2013. Effects of feed and draw solution temperature and transmembrane temperature difference on the rejection of trace organic contaminants by forward osmosis. Journal of Membrane Science 438, 57-64.

Xu, P., Drewes, J.E., Bellona, C., Amy, G., Kim, T.U., Adam, M., Heberer, T., 2005. Rejection of emerging organic micropollutants in nanofiltration-reverse osmosis membrane applications. Water environment research : a research publication of the Water Environment Federation 77, 40-48.

Yoon, Y., Lueptow, R.M., 2005. Removal of organic contaminants by RO and NF membranes. Journal of Membrane Science 261, 76-86.

Zhang, M., Hong, H., Lin, H., Shen, L., Yu, H., Ma, G., Chen, J., Liao, B.-Q., 2018. Mechanistic insights into alginate fouling caused by calcium ions based on terahertz time-domain spectra analyses and DFT calculations. Water Research 129, 337-346.